

# Performance Analysis of Generalized Product Codes with Irregular Degree Distribution

Sisi Miao<sup>†</sup>, Jonathan Mandelbaum<sup>†</sup>, Lukas Rapp<sup>‡</sup>, Holger Jäkel<sup>†</sup>, and Laurent Schmalen<sup>†</sup>

<sup>†</sup>Karlsruhe Institute of Technology (KIT), Communications Engineering Lab (CEL), 76187 Karlsruhe, Germany

<sup>‡</sup>now with Research Laboratory of Electronics (RLE), Massachusetts Institute of Technology, Cambridge, MA 02139 USA

Email: {sisi.miao@kit.edu}

**Abstract**—This paper investigates the theoretical analysis of intrinsic message passing decoding for generalized product codes (GPCs) with irregular degree distributions, a generalization of product codes that allows every code bit to be protected by a minimum of two and potentially more component codes. We derive a random hypergraph-based asymptotic performance analysis for GPCs, extending previous work that considered the case where every bit is protected by exactly two component codes. The analysis offers a new tool to guide the code design of GPCs by providing insights into the influence of degree distributions on the performance of GPCs.

## I. INTRODUCTION

Product codes (PCs) [1] were initially introduced as a 2D array with rows and columns protected by possibly different row and column component codes. Typically, the component codes are Bose–Chaudhuri–Hocquenghem (BCH) or Reed–Solomon (RS) codes, known for their large minimum distances and efficient low-complexity algebraic bounded distance decoding (BDD). Subsequently, through a spatially-coupled structure, PCs were generalized to include staircase codes [2], zipper codes [3], braided codes [4], and many more, resulting in enhanced decoding performance. The shared characteristic of the above-mentioned codes is that each bit is invariably protected by exactly two component codes. Utilizing the concept of generalized low-density parity-check (GLDPC) codes [5], this leads to a Tanner graph with a regular variable node (VN) degree of 2, the minimum value required for iterative decoding.

Apart from spatial coupling, a natural extension of PCs involves considering an increased VN degree, either regular or irregular. A straightforward example is a 3D PC, which offers increased error-correcting capabilities, but also leads to a substantial rise in block length and number of component code decoding steps. Using the zipper code framework, GPCs with high VN degree can be constructed with only a small decoding complexity increase. Recent works have proposed some new generalized zipper codes [6], [7]. We refer to the various generalized codes as generalized product codes (GPCs).

Two approaches exist in the literature to study the asymptotic performance of GPCs. One studies the extrinsic message

passing (EMP) decoding [8] using GLDPC code ensembles and density evolution. Although EMP decoding provides an additional decoding gain compared to intrinsic message passing (IMP), it requires a modified component code decoder with increased decoding complexity and additional storage. The main advantage of the EMP-based analysis is that miscorrections can be handled rigorously. Another approach presented in [9] also studies the decoding behavior of GLDPC ensembles but uses a differential equation method to study the original IMP decoding of GPCs, where the messages passed on a certain edge are *dependent* on the previous messages from the same edge, contrary to EMP.

In this work, we use a different approach to derive a theoretical analysis of the IMP decoding behavior of GPCs extending the previous work of Justesen [10] and Häger et. al. [11] where only GPCs with regular VN degree of 2 is considered. The analysis is based on the theory of random graphs [12], [13] and the asymptotic ensembles of error patterns, where the randomness is introduced by the channel, and no code ensemble is needed. As we study a fixed interleaver defined by specific GPCs, our approach accommodates different decoding schedules and thus, is better suited for spatially-coupled codes typically decoded with a sliding window decoder. We also study an extended version of staircase codes [2] with an irregular degree distribution using both theoretical and simulation results.

**Notation:** Boldface letters denote vectors, matrices, and tensors, e.g.,  $\mathbf{a}$  and  $\mathbf{A}$ . Let  $L^{\times r}$  be the shorthand notation for  $L \times L \times \dots \times L$  with  $r$  occurrences of the number  $L$ . It is used in defining the shape and dimension of a tensor, e.g.,  $\mathbf{A} \in \mathbb{N}^{L^{\times r}}$ . The  $i$ th component of vector  $\mathbf{a}$  is denoted by  $a_i$  and the elements of an  $r$ -dimensional tensor  $\mathbf{A}$  are denoted by  $A_{i_1, i_2, \dots, i_r}$ . The notation  $\mathbf{A}_{:, \dots, :, i, :, \dots, :}$  with  $i$  at the  $j$ th position extracts the  $i$ th slice of  $\mathbf{A}$  along the  $j$ th dimension, yielding a tensor with dimension reduced by 1. The notation  $\mathbf{A}_{:, i: j}$  retrieves columns  $i$  to  $j$  of  $\mathbf{A}$ . Matrix transpose is denoted as  $\mathbf{A}^T$ . The set  $\{1, 2, \dots, p\}$  is denoted by  $[p]$  for any  $p \in \mathbb{N}$ . The Poisson distribution with mean  $\lambda$  is denoted as  $\text{Po}(\lambda)$ , and  $\Psi_{\geq t}(\lambda) = \mathbb{P}(\text{Po}(\lambda) \geq t)$ . For a multiset  $\underline{i}$ , the backslash notation, i.e.,  $\underline{i} \setminus x$ , means removing  $x$  from  $\underline{i}$  once.

## II. GPCs AND RANDOM HYPERGRAPHS

**Definition 1.** A GPC  $\mathcal{C}$  is an extension of a PC where every bit is protected by at least 2 component codes.  $\triangle$

This work has received funding from the European Research Council (ERC) under the European Union's Horizon 2020 research and innovation programme (grant agreement No. 101001899) and from the German Federal Ministry of Education and Research (BMBF) within the project Open6GHub (grant agreement 16KISK010).

Tanner graphs represent the specific structure of GPCs.

**Definition 2.** The *Tanner graph* associated with a GPC is a bipartite graph consisting of a set of  $N$  check nodes (CNs) and a set of  $M$  VNs. Every CN  $(c_i)_{i \in [N]}$  represents a component code and every VN  $(v_j)_{j \in [M]}$  represents a code bit. An edge between CN  $c_j$  and VN  $v_i$  exists if the VN participates in the codeword of the CN. The set of indices of all neighboring CNs of a VN  $v_j$  is denoted as  $\mathcal{N}(v_j)$ . Define  $r_j := |\mathcal{N}(v_j)|$  and  $r_{\max} = \max\{r_j : j \in [M]\}$ . A GPC is *regular* if all VNs have the same degree and otherwise *irregular*.  $\Delta$

Next, Def. 3 encodes the asymptotic structure of GPCs.

**Definition 3.** For a GPC, we divide the set of  $N$  CNs of the GPC into  $I$  disjoint subsets called *positions* labeled from 1 to  $I$ , and define a set of *connection tensors*  $\{\mathbf{A}\} := \{\mathbf{A}^{(2)}, \mathbf{A}^{(3)}, \dots, \mathbf{A}^{(r_{\max})}\}$  such that:

- (1) Each position  $i \in [I]$  contains  $N_i$  CNs and  $\sum_i N_i = N$ . Additionally, we define  $\gamma_i = N_i/N$ .
- (2) For every  $r \in [r_{\max}] \setminus \{1\}$ ,  $\mathbf{A}^{(r)} \in \mathbb{N}_0^{I \times r}$  represents the connection of the CNs via degree  $r$  VNs in the sense that for any  $i_1 \in [I]$  and  $i_2 \leq i_3 \leq \dots \leq i_r$ , every CN at position  $i_1$  is connected to the CNs at position  $i_2, i_3, \dots, i_r$  via  $\mathbf{A}_{i_1, i_2, \dots, i_r}^{(r)}$  degree  $r$  VNs. If  $i_2 \leq i_3 \leq \dots \leq i_r$  is not fulfilled,  $\mathbf{A}_{i_1, i_2, \dots, i_r}^{(r)} = 0$ .  $\Delta$

We illustrate how the connection tensors are obtained. First, the partitioning of the CNs must ensure that all CNs within the same position have the same number of degree  $r$  VNs connecting to any other  $r - 1$  positions for any  $r$ . Therefore, the partition is not arbitrary, but every position should contain “similar” CNs. Then, we consider the subgraph of the Tanner graph consisting of degree  $r$  VNs and their neighboring CNs. The sum of the entries of  $\mathbf{A}_{i_1, i_2, \dots, i_r}^{(r)}$  is the degree of the CNs at position  $i_1$  in this subgraph. The additional restriction, i.e.,  $i_2 \leq i_3 \leq \dots \leq i_r$ , ensures that the number of neighboring VNs to a CN is counted exactly once. Note that a given set of connection tensors permits non-unique Tanner graphs as it only specifies the number of connecting VNs between positions but not the exact connections between single vertices. In contrast to a code ensemble, the connections between the positions can be arbitrary but are fixed. We further clarify this in Examples 1 and 2. Another example will be described later in Sec. V-B.

**Example 1.** For a plain 2D PC with the same row and column component code  $\mathcal{C}_c(n_c, k_c)$ , with an example depicted in Fig. 1-(a), we see that every row CN is connected to the column CNs via  $n$  degree 2 VNs and vice versa. Therefore, we choose  $I = 2$  and  $N_1 = N_2 = n$ , corresponding to the row and column CNs defined as position 1 and 2, respectively. Then,  $\{\mathbf{A}\} = \{\mathbf{A}^{(2)}\}$  where  $\mathbf{A}^{(2)} = \begin{pmatrix} 0 & n \\ n & 0 \end{pmatrix}$ .

**Example 2.** For a 3D cubic PC consisting of the same component code  $\mathcal{C}_c(n_c, k_c)$ , with an example depicted in Fig. 2-(a), we notice that we can subdivide the CNs into positions 1, 2, and 3. These positions correspond to the directions along which a CN is placed, namely, along the  $x$ ,  $y$ , or  $z$ -axis, respectively, resulting in  $I = 3$  and  $N_1 = N_2 = N_3 = n^2$ . We can verify that, e.g., every CN at position 1 is connected to

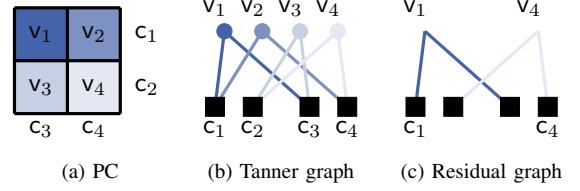


Fig. 1. Graphical illustration of a 2D PC whose component codes are  $(n_c = 2, k_c = 1)$  codes and the process of obtaining the residual graph from its Tanner graph assuming that  $v_1$  and  $v_4$  are erased.

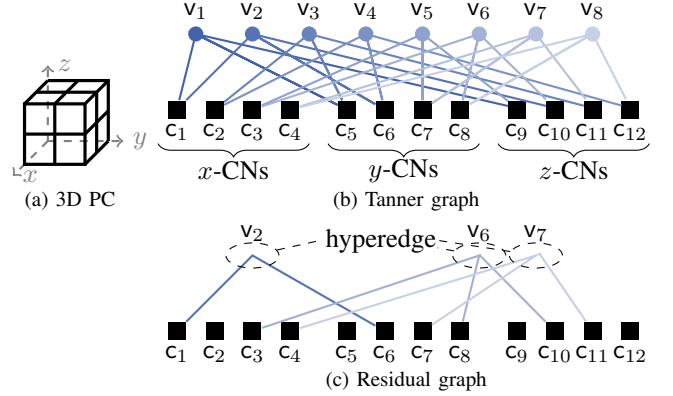


Fig. 2. Graphical illustration of a 3D PC whose component codes are  $(n_c = 2, k_c = 1)$  codes and the process of obtaining the residual graph from its Tanner graph assuming that  $v_2, v_6$ , and  $v_7$  are erased.

$n$  degree 3 VNs, which then connect to  $n$  CNs at position 2 and  $n$  CNs at position 3. The connection tensors are  $\{\mathbf{A}\} = \{\mathbf{A}^{(2)}, \mathbf{A}^{(3)}\}$  where  $\mathbf{A}^{(2)} = \mathbf{0}_{3 \times 3}$  and  $\mathbf{A}^{(3)}$  is

$$\mathbf{A}_{1,2,3}^{(3)} = \begin{pmatrix} 0 & 0 & 0 \\ 0 & 0 & n \\ 0 & 0 & 0 \end{pmatrix}, \mathbf{A}_{2,1,3}^{(3)} = \begin{pmatrix} 0 & 0 & n \\ 0 & 0 & 0 \\ 0 & 0 & 0 \end{pmatrix}, \mathbf{A}_{3,1,2}^{(3)} = \begin{pmatrix} 0 & n & 0 \\ 0 & 0 & 0 \\ 0 & 0 & 0 \end{pmatrix}.$$

**Definition 4.** [14] A *hypergraph*  $(V, E)$  is defined as a set  $V$  of vertices and a set  $E$  of hyperedges, which are subsets of the set of vertices, i.e.,  $E \subseteq \mathcal{P}(V)$ . The *degree* of a hyperedge  $e \in E$  is its cardinality. A hypergraph is *simple* if no hyperedge is a subset of another hyperedge. A hypergraph is termed *r-uniform* if all hyperedges have cardinality  $r$ . A 2-uniform hypergraph is a graph.  $\Delta$

A Tanner graph according to Def. 2 can be described as a hypergraph by choosing the CNs as vertices, i.e.,  $V = \{c_i : i \in [N]\}$ . Then, choosing the neighboring sets of the VNs as the hyperedges of the hypergraph, i.e.,  $E = \{\{c_i : i \in \mathcal{N}(v_j)\} : j \in [M]\}$ . Note that all hypergraphs used in this manuscript are simple. Next, we define residual graphs of a GPC with two examples depicted in Fig. 1 and Fig. 2.

**Definition 5.** Let  $\mathcal{E} \subseteq [M]$  be the set of indices of erased VNs. Then, a residual graph of a GPC is a hypergraph  $(V_R, E_R)$  consisting of the hyperedges associated with erased VNs and the vertices contained these hyperedges, i.e.,  $E_R = \{\{c_i : i \in \mathcal{N}(v_j)\} : j \in \mathcal{E}\}$  and  $V_R = \bigcup_{e \in E_R} e$ .  $\Delta$

Based on [13], [15]–[17], we introduce the following simplified and residual graph-adapted definition.

**Definition 6.** Consider the vertex and hyperedge sets based on the GPC  $\mathcal{C}$  defined as follows:

- (1) Vertices: There exist  $N^G$  vertices, each being independently assigned a *type*  $i \in [I]$  with probability  $\gamma_i$ . Let  $N_i^G := N^G \gamma_i$ .
- (2) Hyperedges: There exist  $m_{\underline{i}_r}$  possible degree  $r$  hyperedges of *type*  $\underline{i}_r$ , where the type  $\underline{i}_r := (i_1, i_2, \dots, i_r)$  is a multiset of the vertex types that the hyperedge contains, i.e., for  $j \in [r], i_j \in [I]$ . Then, a hyperedge is characterized by the tuple  $(r, \underline{i}_r, m_{\underline{i}_r})$ .

A GPC-associated *inhomogeneous random hypergraph* (IRH)  $H(p, \mathcal{C})$  is a probability space where each hyperedge appears independently with probability  $p$  regardless of its type.  $\Delta$

We first focus on a *binary erasure channel* (BEC) with erasure probability  $p$  and GPCs with identical component codes  $\mathcal{C}_c(n_c, k_c, t)$  that recover up to  $t$  erasures each. The iterative decoding process entails the removal of all erasures by the component decoder  $D_c$  if it is connected to up to  $t$  erasures in each iteration.

Comparing Def. 3 and Def. 6 establishes connections between the corresponding concepts. In our analysis, every VN is erased with probability  $p$  and, therefore, every hyperedge appears with probability  $p$  in the IRH. The type of vertices in the IRH corresponds to the positions of a CN in the GPC. The parameters such as  $\gamma_i$  and entries of  $\mathbf{A}^{(r)}$  given by a GPC are used as constants. Then, the IRH analysis is based on the assumption that  $N^G \rightarrow \infty$  while preserving  $N_i^G = N^G \gamma_i$  and

$$m_{\underline{i}_r}/N_{i_j}^G = A_{i_j, \underline{i}_r \setminus i_j}^{(r)} \quad (1)$$

for all  $\underline{i}_r$  and  $i_j \in \underline{i}_r$ . When used as index of a tensor, the multiset  $\underline{i}_r \setminus i_j$  is assumed to be sorted ascendingly.

### III. DECODING EVOLUTION OF GPCs

In this section, we derive Theorem 1, which is a mathematically tractable recursion on the bounded average of the IRH referred to as decoding evolution (DE). To do so, we apply iterative peeling of the branching tree formed in a branching process [18, Chap. 10] of the IRH.

Consider a branching process that begins with a single root vertex at depth  $\ell = 0$  and extends iteratively. Define an offspring hyperedge (OH) as an incident hyperedge of the parent node at depth  $\ell$  which extends to depth  $\ell + 1$  and define the offspring vertices (OVs) as the vertices introduced by the OHs. At every layer  $\ell$ , every vertex generates a random number of OHs where each OH of type  $\underline{i}_r$  introduces  $r - 1$  OVs. The branching process based on our IRH is a discrete-time Markov chain  $(Z_\ell)_{\ell \geq 0}$  defined by  $Z_0 = 1$  and  $Z_{\ell+1} = \sum_{j=1}^{Z_\ell} \xi_{\ell,j}$  representing the number of vertices at level  $\ell + 1$ . Here,  $(\xi_{\ell,j})_{\ell,j \geq 0}$  is a two-dimensional sequence of non-negative integer random variables (RVs) representing the number of OVs of the  $j$ th vertex at depth  $\ell$ . Additionally, we define  $(\zeta_{\ell,j})_{\ell,j \geq 0}$  as non-negative integer RVs representing the number of OHs. To determine the shape of the branching tree, we compute the distribution of  $\zeta_{\ell,j}$ , with which the distribution of  $\xi_{\ell,j}$  is associated. Moreover, as becomes more clear in what follows, the distribution of  $\zeta_{\ell,j}$  determines the DE.

Now, we consider an arbitrary vertex of type  $i \in [I]$  at an arbitrary depth  $\ell$  as a parent vertex. Note that the number of

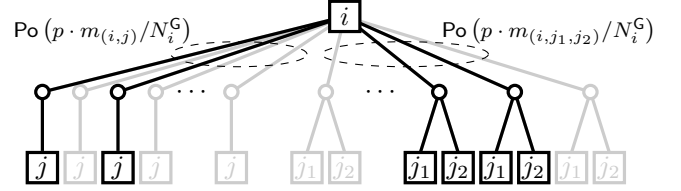


Fig. 3. An example of one level branching process of one vertex of type  $i$ . Vertices are depicted as squares with its type in it. Hyperedges are depicted as a circles connecting the vertices. Possible hyperedges are shown in gray. Hyperedges are realized with probability  $p$  and depicted in black. Assume that the type  $i$  vertex is connected to type  $j$  vertices by degree 2 hyperedges and to type  $j_1$  and  $j_2$  vertices by degree 3 hyperedges.

OHs depends solely on the parent vertex type, irrespective of its depth. Then, the number of its OHs of type  $\underline{i}_r$  follows  $\text{Po}(p \cdot m_{\underline{i}_r}/N_i^G)$  as  $N_i^G \rightarrow \infty$  and the occurrence of every hyperedge is Bernoulli distributed with probability  $p$ . Additionally, the average number of realized OHs is  $p \cdot m_{\underline{i}_r}/N_i^G$ . Define the set of hyperedge types  $\mathcal{I}_{r,i} := \{\underline{i}_r : i \in \underline{i}_r\}$ . Then, using the merging property of Poisson processes, the total number of OHs follows  $\text{Po}(\lambda_i)$  with

$$\lambda_i = \sum_{r=2}^{r_{\max}} \sum_{\underline{i}_r \in \mathcal{I}_{r,i}} p \cdot m_{\underline{i}_r}/N_i^G. \quad (2)$$

An example of the branching from one vertex is illustrated in Fig. 3. Therefore, we write that  $\zeta_{\ell,j} \sim \text{Po}(\lambda_{\tau(Z_j)})$  where  $\tau(Z_j) \in [I]$  maps  $Z_j$  to its vertex type. Repeating the branching process yields a branching tree.

Now, we perform an iterative batch peeling process from depth  $\ell - 1$  to depth 0. In contrast to [11], every peeling step is split into two steps. Starting at depth  $\ell - 1$ , in the first step, given that  $D_c$  corrects up to  $t$  erasures, all vertices at depth  $\ell - 1$  are peeled if the number of their incident hyperedges is at most  $t$ , including its OHs and the hyperedge extending to its parent vertex at depth  $\ell - 2$ . We compute  $x_i^{(1)} = \Psi_{\geq t}(\lambda_i)$  to be the probability of a vertex at depth  $\ell - 1$  and in position  $i$  surviving the peeling. In the second step, before proceeding to depth  $\ell - 2$ , we remove all hyperedges connecting depth  $\ell - 2$  to  $\ell - 1$  if they involve any peeled vertex. The interpretation is that a bit is recovered (meaning its associated hyperedge is removed) if it is recovered by any of its component decoders. Using the splitting property of Poisson processes, we know that the number of surviving OHs of a type  $i$  vertex at depth  $\ell - 2$  is now  $\text{Po}(\lambda_i \prod_{i_j \in \underline{i}_r \setminus i} x_{i_j}^{(1)})$  distributed. The process is repeated yielding the update equation  $x_i^{(\ell+1)} = \Psi_{\geq t}(\lambda_i \prod_{i_j \in \underline{i}_r \setminus i} x_{i_j}^{(\ell)})$ . Together with (1) and (2), we obtain Theorem 1.

**Theorem 1.** For a GPC, let  $\mathbf{x}^{(\ell)} = (x_1^{(\ell)} \ x_2^{(\ell)} \ \dots \ x_I^{(\ell)})$  and  $x_i^{(\ell)}$  corresponds to the probability that a bit at position  $i \in [I]$  is not recovered after  $\ell$  decoding iterations by any of its component codes estimated by its associated IRH assuming  $N^G \rightarrow \infty$ . With  $\mathbf{x}^{(0)} = \mathbf{1}_{1 \times I}$ , the evolution of  $\mathbf{x}^{(\ell)}$  is characterized as

$$x_i^{(\ell+1)} = \Psi_{\geq t} \left( p \cdot \sum_{r=2}^{r_{\max}} \sum_{\underline{i}_r \in \mathcal{I}_{r,i}} A_{i, \underline{i}_r \setminus i}^{(r)} \prod_{i_j \in \underline{i}_r \setminus i} x_{i_j}^{(\ell)} \right). \quad (3)$$

#### IV. DECODING SCHEDULE

Comparing to the code ensemble based methods [8], [9], the advantage of the random graph-based analysis is the ability to incorporate certain decoding schedules. This is especially beneficial for spatially coupled GPCs, where a windowed decoder is used instead of global decoding and also when considering the position-alternating nature of GPC decoding. For example, for the 2D PC defined in Example 1, assume that decoding starts with the row CNs at position  $i = 1$ . Therefore, when decoding the column codes, the row codes have undergone one additional decoding step. The decoding evolution adapts by computing  $x_2^{(\ell+1)}$  using the updated  $x_1^{(\ell+1)}$  while computing  $x_1^{(\ell+1)}$  using  $x_2^{(\ell)}$ .

Let  $\mathcal{W}$  denote the positions that are decoded in the current window and arrange the  $I$  positions such that position  $i_1$  is decoded before position  $i_2$  if  $i_1 < i_2$ . The decoding evolution is modified to

$$x_i^{(\ell+1)} = \begin{cases} \Psi_{\geq t} \left( p \sum_{r=2}^{r_{\max}} \sum_{\mathbf{i}_r \in \mathcal{I}_{r,i}} A_{i, \mathbf{i}_r}^{(r)} \prod_{\substack{i_j \in \mathbf{i}_r \setminus i, \\ i_j \geq i}} x_{i_j}^{(\ell)} \prod_{\substack{i_j \in \mathbf{i}_r \setminus i, \\ i_j < i}} x_{i_j}^{(\ell+1)} \right) & i \in \mathcal{W} \\ x_i^{(\ell)} & i \notin \mathcal{W}. \end{cases}$$

#### V. APPLICATIONS OF THE DE

We apply the derived DE to binary symmetric channels (BSCs)—where GPCs are widely used—altering the meaning of  $p$  and  $t$ . Hereafter,  $p$  denotes the cross-over probability of a BSC and  $t$  is the number of errors  $D_c$  can correct. Our conclusion on the BEC naturally transfers to the BSC assuming an idealized  $D_c$  correcting up to  $t$  errors without any *miscorrections*—instances where  $D_c$  yields a codeword  $c \in \mathcal{C}_c$  but  $c \neq x$ , the transmitted codeword. The decoder is referred to as miscorrection-free (MF) iterative BDD (iBDD). The MF assumption does not hold for most of the practically used GPCs, which often use component codes with small minimum distance and hence  $t$ . However, MF decoding can be approached using, e.g., extensive component code shortening [6], [19], anchor decoding [20], or soft-aided decoding algorithms [21], [22], which are beyond the scope of this work.

##### A. Bit Error Rate (BER) Prediction

The BER predicted by DE after  $L$  decoding iterations is

$$p \cdot \frac{\sum_{r=2}^{r_{\max}} \sum_{\mathbf{i}_r \in \mathcal{I}_{r,i}} A_{i, \mathbf{i}_r}^{(r)} \prod_{i_j \in \mathbf{i}_r} x_{i_j}}{\sum_{r=2}^{r_{\max}} \|A^{(r)}\|},$$

where  $x := x^{(L)}$  and  $\|A^{(r)}\|$  is the sum of the values of the elements of  $A^{(r)}$ . As an example, Fig. 4 compares the DE results with simulated BER results after MF iBDD decoding for the cubic PC with  $(127, 113, 2)$  BCH component codes using different number of decoding iterations  $L$ . The theoretical and simulated results closely agree.

##### B. Extended Staircase Code with DE

We construct and inspect a simple extended staircase code (ESC), a generalized zipper code [3] with flexible degree distribution, to obtain insights on the influence of the degree distribution on the decoding performance.

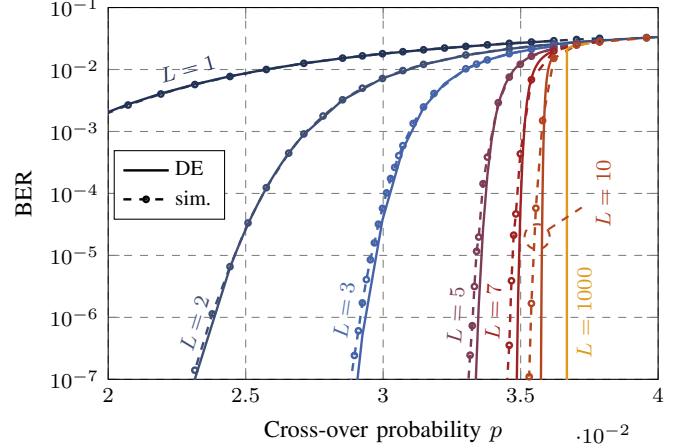


Fig. 4. DE and simulation results of the 3D PC with  $(127, 113, 2)$  BCH component codes using  $L$  iterations of MF iBDD decoding over a BSC.

1) *Code Construction*: A zipper code can be described in an infinite buffer of width  $n_c$  where every row is protected by a component code  $\mathcal{C}_c(n_c, k_c)$ . The buffer consists of the real part  $B$  to be transmitted over the channel and the virtual part  $V$  obtained from  $B$  via a specific mapping. To describe an ESC, we divide every  $\omega$  rows of the buffer into one spatial position indicated by a subscript  $i \in \mathbb{N}$ , e.g.,  $B_i$  and  $V_i$ . Additionally, define a configurable parameter  $\kappa$ .

Upon encoding, one block  $B_i \in \mathbb{F}_2^{\omega \times \omega}$  is generated at a time where  $(B_i)_{:,1:(k_c-\omega-\kappa)}$  are new information bits and  $(B_i)_{:, (k_c-\omega-\kappa+1):\omega}$  are parity check bits obtained by encoding the rows at spatial position  $i$ . To do so, we partition  $V_i = \begin{pmatrix} V_i^{(1)} & V_i^{(2)} \end{pmatrix} \in \mathbb{F}_2^{\omega \times (\kappa+\omega)}$  for all  $i$  and define the mapping as  $V_{i+1}^{(2)} = B_i^T \in \mathbb{F}_2^{\omega \times \omega}$  and  $V_{i+3}^{(1)} = (B_i)^{P, \kappa} \in \mathbb{F}_2^{\omega \times \kappa}$  where the operator  $(X)^{P, \kappa}$  is a cyclic permutation of the first  $\kappa$  columns of  $X$ , i.e.,  $(X^{P, \kappa})_{((i+j-1) \bmod \omega)+1, j} = X_{i, j}$  for  $j \in [\kappa]$ . The mappings are defined to fulfill the general rule of thumb for mitigating high error floors by avoiding any two bits appearing in the same row more than once. A more extensive study of the mappings is presented in [7].

To match a design code rate  $R$ , we choose a real buffer width  $\omega$  such that  $\frac{\omega - (n_c - k_c)}{\omega} = R$ , regardless of the degree distribution. To ensure an integer number of bits,  $\omega$  is rounded to the nearest integer, causing a negligible deviation from  $R$ . We can then construct ESCs with different degree distributions for the same code rate  $R$ . We use a  $(2^\nu, 2^\nu - t\nu, t)$  extended BCH code and shorten it such that  $n_c = \kappa + 2\omega$ . To have a valid ESC,  $\omega > t\nu$ ,  $2\omega + \kappa \leq 2^\nu$  and  $0 \leq \kappa \leq \omega$  must hold. When  $\kappa = 0$ , the code is a staircase code. When  $\kappa = \omega$ , the code is a regular generalized zipper code with VN degree 3. The structure of the ESC is depicted in Fig. 5 where dark and light-colored parts consists of degree 3 and degree 2 VNs, respectively.

We proceed to the connection tensors of the ESC. First, the positions are obtained by partitioning every spatial position  $i$  into two positions  $i_u$  and  $i_l$  containing the first  $\kappa$  rows and the last  $\omega - \kappa$  rows, respectively. Then, for an ESC

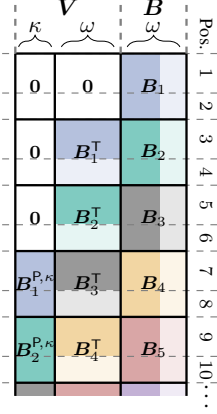


Fig. 5. Graphical illustration of the ESC.

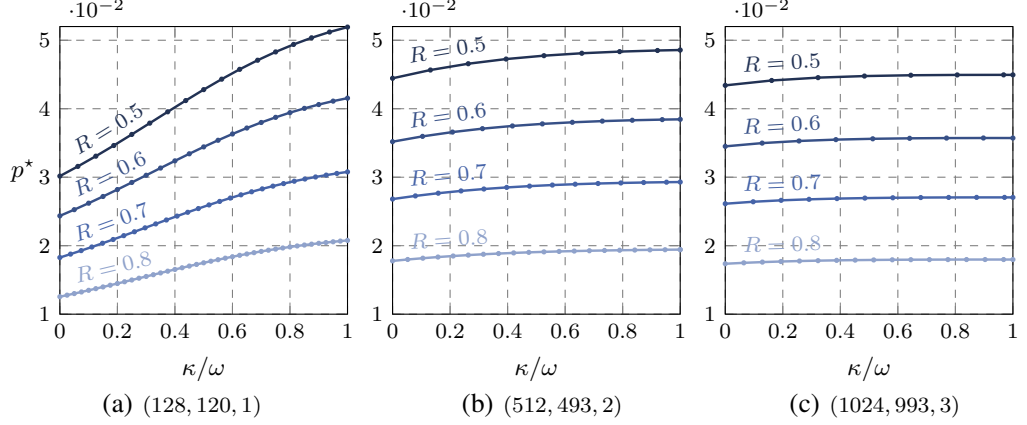


Fig. 6. Decoding thresholds  $p^*$  for ESCs of different rates  $R$  based on (a) (128, 120, 1), (b) (512, 493, 2), and (c) (1024, 993, 3) extended BCH component codes using DE.

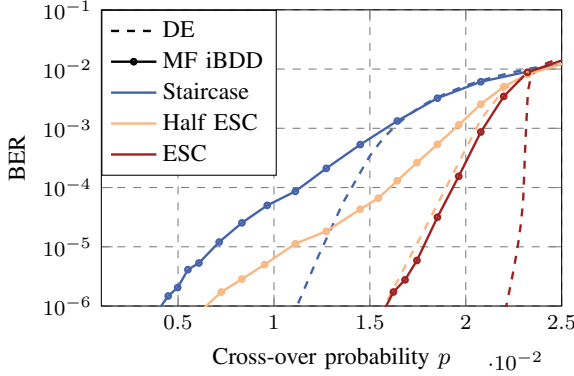


Fig. 7. Decoding results of the ESC based on (128, 120, 1) extended BCH component codes. The ESC rate is 0.77 with  $\omega = 35$ . We select  $\kappa = 0, 18$ , and 35, corresponding to staircase, half ESC, and ESC code, respectively.

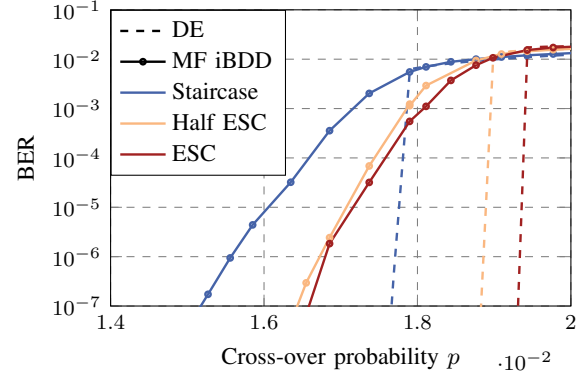


Fig. 8. Decoding results of the ESC based on (512, 493, 2) extended BCH component codes. The ESC rate is 0.8 with  $\omega = 95$ . We select  $\kappa = 0, 50$ , and 95, corresponding to staircase, half ESC, and ESC code, respectively.

with  $I'$  spatial positions, we have  $I = 2I'$ ,  $N_{2i-1} = \kappa$ , and  $N_{2i} = \omega - \kappa$  for all  $i \in [I']$ . Naturally,  $\mathbf{A} = \{\mathbf{A}^{(2)}, \mathbf{A}^{(3)}\}$  as  $r_{\max} = 3$ . We first compute the entries of  $\mathbf{A}^{(2)}$ . For odd  $i$  and  $i \in [I - 3]$ , we have  $A_{i,i+3}^{(2)} = \omega - \kappa$  and  $A_{i+3,i}^{(2)} = \kappa$ . For even  $i$  and  $i \in [I - 2]$ , we have  $A_{i,i+2}^{(2)} = A_{i+2,i}^{(2)} = \omega - \kappa$ . We then compute the entries of  $\mathbf{A}^{(3)}$  using an approximation that the bits in the upper and lower parts of  $\mathbf{V}_i^{(1)}$  are treated as identical for all  $i$ .<sup>1</sup> Then, for odd  $i$  and  $i \in [I - 6]$ , we have  $A_{i,i+2,i+6}^{(3)} = A_{i+2,i,i+6}^{(3)} = A_{i+6,i,i+2}^{(3)} = \kappa$ . For even  $i$  and  $i \in [I - 6]$ , we have  $A_{i,i+1,i+6}^{(3)} = A_{i+6,i,i+1}^{(3)} = \kappa$  and  $A_{i+1,i,i+6}^{(3)} = \omega - \kappa$ . All other entries of  $\mathbf{A}^{(2)}$  and  $\mathbf{A}^{(3)}$  are 0.

2) *Results:* The impact of the degree distribution on the decoding performance of ESCs is examined using a fixed window length of 7 and 8 decoding iterations. The decoding threshold  $p^*$  denotes the minimum  $p$  value for which the DE-estimated BER falls below  $10^{-4}$ . Consistently, an increase in the fraction of degree 3 VNs leads to an improvement in the decoding threshold, with greater improvements observed as  $t$  decreases. Notably, for the rarely used  $t = 1$  codes, introducing high-degree VNs results in the most significant improvement. Figure 6 depict the results of  $p^*$  for three ESC

families based on the (128, 120,  $t = 1$ ), (512, 493,  $t = 2$ ), and (1024, 993,  $t = 3$ ) extended BCH codes. Similar trends are observed for other component codes with various lengths.

Based on the observations of decoding thresholds, we take a closer look on two sets of exemplary codes based on (128, 120, 1) and (512, 493, 2) extended BCH codes using MF iBDD, as depicted in Fig. 7 and Fig. 8, respectively. The post-decoding BER improvements achieved by leveraging high-degree VNs align with the DE predictions. Particularly, for the  $t = 1$  code, a substantial decoding gain is observed, while for the  $t = 2$  code, introducing approximately 50% degree 3 VNs leads to noticeable improvements. Furthermore, beyond the decoding threshold improvement, we heuristically deduce that high-degree ESCs exhibit a lower error floor compared to staircase codes. This aligns with observations in [6] and [7], although a systematic error floor analysis of irregular GPC has not been conducted. Note that in practice, MF iBDD can be approached using the aforementioned methods [6], [19]–[22].

## VI. CONCLUSION

We analyze the asymptotic decoding behavior of GPCs with irregular degree distribution through the derived decoding evolution. As an example, we examine a simple extension of the staircase code. Future work includes, e.g., extending the analysis to a mixture of different component codes.

<sup>1</sup>Such approximation is often needed when handling GPCs where the interleaving of the bits are relatively complex, e.g., the Chevrone codes [6]. However, a good alignment of the DE and simulated results is still observed.

## REFERENCES

- [1] P. Elias, "Coding for noisy channels," in *IRE Convention Record, Part IV*, Mar. 1955, pp. 37–46.
- [2] B. P. Smith, A. Farhood, A. Hunt, F. R. Kschischang, and J. Lodge, "Staircase codes: FEC for 100 Gb/s OTN," *J. Lightw. Technol.*, vol. 30, no. 1, pp. 110–117, 2011.
- [3] A. Y. Sukmadji, U. Martínez-Peñas, and F. R. Kschischang, "Zipper codes," *J. Lightw. Technol.*, vol. 40, no. 19, pp. 6397–6407, 2022.
- [4] A. J. Feltström, D. Truhachev, M. Lentmaier, and K. S. Zigangirov, "Braided block codes," *IEEE Trans. Inf. Theory*, vol. 55, no. 6, pp. 2640–2658, 2009.
- [5] R. M. Tanner, "A recursive approach to low complexity codes," *IEEE Trans. Inf. Theory*, vol. 27, no. 5, pp. 533–547, Sep. 1981.
- [6] A. Y. Sukmadji, F. R. Kschischang, and M. Shehadeh, "Generalized spatially-coupled product-like codes using zipper codes with irregular degree," in *Proc. IEEE Global Telecommun. Conf. (GLOBECOM)*, 2023.
- [7] M. Shehadeh, F. R. Kschischang, and A. Y. Sukmadji, "Higher-order staircase codes," *arXiv preprint arXiv:2312.13415*, 2023.
- [8] Y.-Y. Jian, H. D. Pfister, and K. R. Narayanan, "Approaching capacity at high rates with iterative hard-decision decoding," *IEEE Trans. Inf. Theory*, vol. 63, no. 9, pp. 5752–5773, 2017.
- [9] L. M. Zhang, D. Truhachev, and F. R. Kschischang, "Spatially coupled split-component codes with iterative algebraic decoding," *IEEE Trans. Inf. Theory*, vol. 64, no. 1, pp. 205–224, 2017.
- [10] J. Justesen, "Performance of product codes and related structures with iterated decoding," *IEEE Trans. Commun.*, vol. 59, no. 2, pp. 407–415, 2010.
- [11] C. Häger, H. D. Pfister, A. Graell i Amat, and F. Brännström, "Density evolution for deterministic generalized product codes on the binary erasure channel at high rates," *IEEE Trans. Inf. Theory*, vol. 63, no. 7, pp. 4357–4378, 2017.
- [12] P. Erdős and A. Rényi, "On random graphs I," *Publ. math. debrecen*, vol. 6, no. 290–297, p. 18, 1959.
- [13] B. Bollobás and O. Riordan, "Random graphs and branching processes," in *Handbook of large-scale random networks*. Springer, 2009, pp. 15–115.
- [14] C. Berge, *Graphs and hypergraphs*. North-Holland Publishing Company Amsterdam, 1973, vol. 7.
- [15] B. Söderberg, "General formalism for inhomogeneous random graphs," *Physical Review E*, vol. 66, no. 6, p. 066121, 2002.
- [16] B. Bollobás, S. Janson, and O. Riordan, "The phase transition in inhomogeneous random graphs," *Random Structures & Algorithms*, vol. 31, no. 1, pp. 3–122, 2007.
- [17] —, "Sparse random graphs with clustering," *Random Structures & Algorithms*, vol. 38, no. 3, pp. 269–323, 2011.
- [18] N. Alon and J. H. Spencer, *The probabilistic method*. John Wiley & Sons, 2016.
- [19] L. M. Zhang and F. R. Kschischang, "Staircase codes with 6% to 33% overhead," *J. Lightw. Technol.*, vol. 32, no. 10, pp. 1999–2002, 2014.
- [20] C. Häger and H. D. Pfister, "Approaching miscorrection-free performance of product codes with anchor decoding," *IEEE Trans. Commun.*, vol. 66, no. 7, pp. 2797–2808, 2018.
- [21] Y. Lei, B. Chen, G. Liga, X. Deng, Z. Cao, J. Li, K. Xu, and A. Alvarado, "Improved decoding of staircase codes: The soft-aided bit-marking (SABM) algorithm," *IEEE Trans. Commun.*, vol. 67, no. 12, pp. 8220–8232, 2019.
- [22] S. Miao, L. Rapp, and L. Schmalen, "Improved soft-aided decoding of product codes with dynamic reliability scores," *J. Lightw. Technol.*, vol. 40, no. 22, pp. 7279–7288, 2022.